A Kalman tracker for super-resolution PIV

Article *in* Experiments in Fluids · April 2012

DOI: 10.1007/s003480070005

4 authors, including:

Ronald J. Adrian
Arizona State University
384 PUBLICATIONS **33,765** CITATIONS

SEE PROFILE

Kenneth T. Christensen
Illinois Institute of Technology
197 PUBLICATIONS **4,771** CITATIONS

SEE PROFILE

Experiments in Fluids [Suppl.] S34–S41 © Springer-Verlag 2000

A Kalman tracker for super-resolution PIV

K. Takehara, R. J. Adrian, G. T. Etoh, K. T. Christensen

Abstract We describe a new super-resolution method of particle-image velocimetry (PIV) based on Kalman filtering and χ^2-testing. Performance of the "super-resolution KC" method is evaluated by Monte-Carlo simulation and by applying the method to measurements of flow fields recorded in the form of double-pulse/single-frame and single-pulse/double-frame particle images. When the images have good contrast, and depending on the intensity of the velocity gradients present in the flow, the super-resolution KC method is able to extract valid measurements from 80 to 100% of the available image pairs. In these tests, the vector yield is increased by more than five times compared to standard PIV analysis.

1 Introduction

PIV measures two- or three-dimensional velocity fields by analyzing displacements of tracer-particle images. Fundamentally, PIV methods are divided into two categories based on the method used to extract the velocity fields from the particle images: pattern-matching velocimetry (PMV) and particle-tracking velocimetry (PTV). PMV estimates velocity fields by tracking patterns of particles in a small interrogation area, while PTV estimates velocity fields by tracking individual particle images.

PMV is able to measure the velocity field from images at two times, whereas PTV commonly relies upon images at more than two instants to improve the reliability of correctly associating particle pairs. On the other hand, the spatial resolution of PTV is higher than that of PMV because the maximum spatial resolution of PMV is equal to the interrogation area. Therefore, in order to obtain reliable measurements, the interrogation region must contain many particles. For example, Keane and Adrian (1992) show that cross-correlation analysis, the most common implementation of PMV, requires, on average, between 5 and 20 particles per interrogation spot. Thus, in principle, PTV can measure 5–20 times more vectors than PMV. In practice, however, PTV fails to achieve this yield if the particles are too close together, leading to ambiguities in the pairing of particle images.

The notion of super-resolution analysis was proposed by Keane et al. (1995) to improve the spatial resolution of PIV by combining the advantages of PMV with those of PTV. Super-resolution analysis was defined as a method which measured the velocity vector of each particle in two time-steps by first performing a standard PIV correlation analysis and then using the resulting velocity-field estimate to guide the particle-image pairing necessary for successful particle tracking. Various forms of particle tracking are encompassed by this scheme. It is one of the more sophisticated PIV algorithms.

Hart (1998) proposed a new algorithm for high-resolution analysis by using recursive local correlation. Subsequent to a standard PIV correlation analysis, the interrogation area is divided into smaller areas and each divided area is re-interrogated in the same manner as a standard correlation PIV, except that the second window is centered on the displacement determined by the previous correlation. The operation is repeated until the size of the interrogation area becomes the minimum size that is equivalent to the individual particle-image size. In this way, there is no need to introduce a new method for the particle-tracking phase of the super-resolution analysis.

Etoh and Takehara (1989, 1995) proposed a PTV algorithm which consists of the Kalman filter and χ^2-test applied to a sequence of PIV images. The particle information at the next time step ($t = t + \Delta t$), such as a location, size, peak brightness, etc., is predicted by a Kalman filter from the information available at the present time ($t = t$). To identify the same particle between adjacent time-steps, the probability of two images belonging to the same particle is judged by a χ^2-test. The KC method is designed for single-pulse/multi-frame PTV, and it is robust when there is a sequence of images from which the Kalman filter can learn. However, by itself it is not well suited to sequences of only two images.

The χ^2 values for the particle information predicted via the Kalman filter and the measured particle information are calculated in a certain interrogation area. The particle-image pair that has a minimum χ^2 value in the interrogation area is temporarily determined as the same particle-image pair. The χ^2 test judges the probability of success of temporarily identified particle-image pairs in successive images by a certain criterion. For instance, when the

K. Takehara (✉), G. T. Etoh
Department of Civil Engineering
Kinki University, Japan

R. J. Adrian, K. T. Christensen
Laboratory for Turbulence and Complex Flow
Department of Theoretical and Applied Mechanics
University of Illinois, Urbana, Illinois 61801, USA

This research was supported in part by the DARPA Microflumes Program.

minimum χ^2 value of a temporarily-identified particle-image pair exceeds a certain rejection criterion, the particle-image pair is judged as incorrect.

This paper presents a new algorithm for super-resolution analysis which consists of correlation PIV and the KC method of PTV. To improve the accuracy of measuring the displacement between image pairs, the particle mask correlation (PMC) method is also employed. The combination of PMV and PTV has the following advantages compared with a standard PIV or PTV analysis:

1. It achieves higher spatial resolution than standard correlation PIV
2. It requires images at only two times, double-pulse/single-frame or single-pulse/double-frame, even at high particle-image density.

While other PTV algorithms can also trace particle movement in two time-steps, they tend to correlate wrong particle pairs when the particle-image density becomes large. For these algorithms, the number of successive frames has to be increased to achieve successful operation for high image densities. Unfortunately, the possibility of recording multiple frames in rapid succession is severely limited by current laser technology. On the other hand, the super-resolution KC method takes longer to analyze a velocity field compared to standard correlation PIV or PTV methods. The time per vector is increased by the computations required for the additional PTV step, and the total time is increased by the increased number of vectors that are obtained. The latter is not unexpected. The performance of the proposed super-resolution KC method is tested with simulated particle images. It is also tested on double-pulse/single-frame images and a single-pulse/double-frame image set from a high turbulence intensity Rushton turbine flow field.

2 Procedure

2.1 Kalman–χ^2 method

Generally, the discrete linear dynamic system is expressed by the following transition equation (Eq. (1)) and observation equation (Eq. (2)):

$$h(t+\Delta t) = \phi(t+\Delta t|t)h(t) + \xi(t+\Delta t) \tag{1}$$

$$m(t) = D(t)h(t) + \zeta(t) \tag{2}$$

where $h(t)$ is a vector of state variables at time t, $m(t)$ is a vector of observation variables at time t, $\phi(t+\Delta t|t)$ is the transition matrix, $D(t)$ is the observation matrix, and $\xi(t)$ and $\zeta(t)$ are vectors of noise for the transition equation (1) and the observation equation (2), respectively. The interested reader should consult standard texts on the subject for a more comprehensive discussion.

In Kalman filtering theory, the least-squares estimate of the state vector $h(t)$ is successively estimated from the observation vector $m(t)$ at each step to predict $h(t+\Delta t|t)$, the optimum estimate of the state variables in the next step. The successive calculation algorithm is expressed as follows:

$$K(t) = P(t|t-\Delta t)D^T(t)\left[D(t)P(t|t-\Delta t)D^T(t) + R(t)\right]^{-1} \tag{3a}$$

$$\hat{h}(t|t) = \hat{h}(t|t-\Delta t) + K(t)\left[m(t) - D(t)\hat{h}(t|t-\Delta t)\right] \tag{3b}$$

$$\hat{h}(t+\Delta t|t) = \phi(t+\Delta t|t)\hat{h}(t|t) \tag{3c}$$

$$P(t|t) = P(t|t-\Delta t) - K(t)D(t)P(t|t-\Delta t) \tag{3d}$$

$$P(t+\Delta t|t) = \phi(t+\Delta t|t)P(t|t)\phi^T(t+\Delta t|t) + Q(t) \tag{3e}$$

where $P(t)$ is the covariance matrix of $(h(t) - \hat{h}(t|t))$ [the difference between the true value and the estimated state variables $h(t)$], $Q(t)$ is the variance matrix of the error in the system equations, and $R(t)$ is the variance matrix of the error in observation equations. The notation $\hat{h}(t)$ refers to the *optimal* estimate of $h(t)$.

In this method, the following equation is applied as the transition equation:

$$\begin{aligned} h(t+\Delta t) &= h(t) + \Delta t \frac{\mathrm{d}h}{\mathrm{d}t}\bigg|_{t=t} + \mathrm{o}\left(\Delta t^2\right) \\ &\cong h(t) + \Delta h(t) + \xi(t) \end{aligned} \tag{4}$$

The observation equation is

$$H(t) = h(t) + \zeta(t) \tag{5}$$

where $H(t)$ is the observed value of $h(t)$. In this study, the X–Y locations of the particle images, the particle-image size and the differences between the time steps are chosen as state variables. For example, the transition equation and the observation equation for the X-location would be written as

$$\begin{Bmatrix} X(t+\Delta t) \\ \Delta X(t+\Delta t) \end{Bmatrix} = \begin{pmatrix} 1 & 1 \\ 0 & 1 \end{pmatrix} \begin{Bmatrix} X(t) \\ \Delta X(t) \end{Bmatrix} + \begin{Bmatrix} \xi_X(t) \\ \xi_{\Delta X}(t) \end{Bmatrix} \tag{6}$$

$$\begin{Bmatrix} \hat{X}(t) \\ \Delta\hat{X}(t) \end{Bmatrix} = \begin{pmatrix} 1 & 0 \\ 0 & 1 \end{pmatrix} \begin{Bmatrix} X(t) \\ \Delta X(t) \end{Bmatrix} + \begin{Bmatrix} \zeta_X(t) \\ \zeta_{\Delta X}(t) \end{Bmatrix} \tag{7}$$

where $X(t)$ is the X-location of the particle image in the image-plane coordinates at time t, $\Delta X(t)$ is the displacement of the particle image following time t, and $\{\hat{X}(t), \Delta\hat{X}(t)\}$ are the observation variables of $\{X(t), \Delta\mathbf{X}(t)\}$.

The particle information predicted by Kalman filtering is compared to the same particle information measured at the next step by means of the χ^2-test. The χ^2-test judges the probability of the combination of the estimated image and measured image being correctly paired and is expressed as

$$\chi^2 = \frac{(X_{\mathrm{mes}} - X_{\mathrm{est}})^2}{\sigma_X^2} + \frac{(Y_{\mathrm{mes}} - Y_{\mathrm{est}})^2}{\sigma_Y^2} + \frac{(d_{\mathrm{mes}} - d_{\mathrm{est}})^2}{\sigma_d^2} + \cdots \tag{8}$$

Since the particle data is only recorded at two time-steps, some modifications to the original KC method reported in Etoh and Takehara (1995) are necessary. Basically, the KC method improves the accuracy of the estimated state

variables by observing and predicting particle information over a number of time-steps. If there are wrong particle pairings made in the first step, the pairs would be automatically eliminated after several steps because the probability of the wrong particle pairs remaining after several steps becomes extremely small. In the present implementation, the original KC is modified as follows:

1. Particle information at the second step is predicted from the interpolated particle information at first time by Kalman filtering.
2. The same particle pair is matched by using the χ^2-test.
3. For unmatched particle pairs, the particle information is interpolated from the information of matched particle pairs using the following equations:

$$\Delta X_P(X,Y) = \frac{\sum_{i=1}^{N} \Delta X_{Gi}(X_{Gi},Y_{Gi}) \cdot w_i(X_{Gi}-X, Y_{Gi}-Y)}{\sum_{i=1}^{N} w_i(X_{Gi}-Y, X_{Gi}-Y)} \quad (9)$$

$$w_i(X_i, Y_i) = \exp\left\{-\frac{X_i^2 + Y_i^2}{\sigma^2}\right\} \quad (10)$$

4. For matched particle pairs, the particle information is also interpolated from the particle information of surrounding matched particle pairs.
5. The particle information of the second time-step is predicted from the measured particle information at the first time.
6. Processes 2–5 are repeated until the number of matched particle is maximized.

2.2 Particle mask correlation method

In the particle mask correlation (PMC) method (Takehara and Etoh 1999) the particle mask serves as a template of the brightness pattern of a typical particle image. Over most of its area, the intensity distribution of a focused particle image is well approximated by a two-dimensional Gaussian distribution (Adrian and Yao 1984). Hence, the mask is assumed to be a Gaussian distribution of the form

$$G(X_i - X_0, Y_i - Y_0) = b \exp\left\{-\frac{(X_i - X_0)^2 + (Y_i - Y_0)^2}{\sigma^2}\right\} \quad (11)$$

where b is the peak brightness, (X_0, Y_0) is the center of a template, and σ is the e^{-1} radius. The correlation coefficients between each particle in the image plane and the particle mask are calculated as

$$C(X_0, Y_0) = \frac{\sum_{X_i=-M/2}^{M/2} \sum_{Y_i=-N/2}^{N/2} (I(X_i, Y_i) - I_{\text{ave}})(G(X_i - X_0, Y_i - Y_0) - G_{\text{AV}})}{\left(\sum_{X_i=-M/2}^{M/2} \sum_{Y_i=-M/2}^{M/2} (I(X_i, Y_i) - I_{\text{AV}})^2\right)^{1/2} \left(\sum_{X_i=-M/2}^{M/2} \sum_{Y_i=-N/2}^{N/2} (G(X_i - X_0, Y_i - Y_0) - G_{\text{AV}})^2\right)^{1/2}} \quad (12)$$

where $C(x_0,y_0)$ is a correlation coefficient at (x_0,y_0), $I(X_i,Y_i)$ is the brightness value of an image at (X_i,Y_i), I_{AV} is the average brightness in the interrogation area, $G(X_i,Y_i)$ is a brightness value of the particle mask at (X_i,Y_i), G_{AV} is the average brightness of the particle mask, and M and N are the size of the interrogation area in the X- and Y-directions, respectively. The correlation coefficients are calculated at all pixels in the image plane. Thus, a correlation plane (X_0,Y_0) corresponding to the image plane is produced.

In order to reject non-particle images, the correlation coefficients are "clipped" at a threshold value. It is found that a value of 0.7 for the correlation coefficient discriminates effectively against linear image elements such as the edge of a water tank or a water surface. The advantages of the PMC method are: (1) very dim particle images, such as out-of-focus particle images, can be extracted from the images because the correlation coefficients depend only on the shape of the brightness pattern; (2) linear elements, such as flow boundaries, are automatically eliminated; and (3) the separation of closely-located particles is better than that achieved by the binarization of the particle-image brightness. Disadvantages of the PMC method include: (1) it is sensitive to noise; and (2) saturated particle images cannot be picked up because their intensity distributions are quite different from the two-dimensional Gaussian distribution assumed by PMC.

2.3 Flowchart of the super-resolution KC method

The flowchart shown in Fig. 1 summarizes the following procedure:

1. A velocity field is calculated on a regular grid using standard correlation PIV analysis, either cross-correlation or auto-correlation. This analysis provides an estimate of the velocity field.
2. Individual particle images are identified and located using the PMC method.
3. From the results of (1) and (2), the velocity of each particle is found by interpolation using Eqs. (9) and (10).
4. The modified KC method is used to estimate the individual particle movement. The result of (3) is used as the initial value for the KC method.

This method can be applied to both single-pulse/double-frame images and double-pulse/single-frame images. In single-pulse/double-frame imaging, the initial velocity of each particle is interpolated for particles present in the first image. Then a correspondence is made between each particle on the first image and each particle on the second

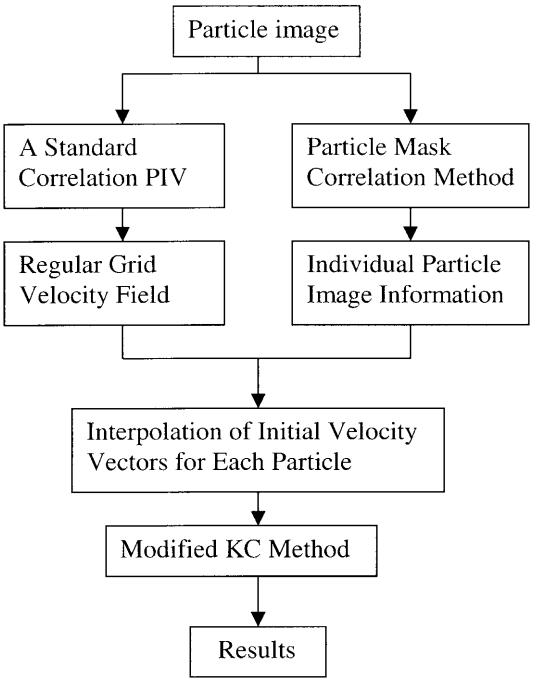

Fig. 1. Flow chart of the super-resolution Kalman tracker algorithm

image. In double-pulse/single-frame imaging, each particle velocity is determined from interpolation of the regular grid data. There is no information about the time at which a particle image is recorded, and further, sometimes two particle pairs are found for one particle. Thus, the particle-image pair that has the minimum χ^2-value is denoted as belonging to the same particle.

3 Performance

3.1 Simulated images

The performance of the super-resolution KC method was tested with simulated particle images. The simulated images were created in the same manner as those used by Keane et al. (1995). Specifically, Monte Carlo simulation was used to locate particles randomly on a double-pulse/single-frame image. The intensity distribution of each particle image is an eight-pixel diameter, two-dimensional Gaussian distribution whose peak brightness value is fixed at 250. Since the mean image diameter is greater than two pixels wide, the bias error introduced by pixelization is small (Prasad et al. 1992). The particle-image density, N_I, defined as the mean number of particles in an interrogation volume, is varied from 10 to 60, and the images have no background noise. The size of the artificially-generated images are 1280 × 1280 pixels, and the size of the PIV interrogation spot, d_I, was fixed at 256 × 256 pixels. The vector field is calculated on a regular grid with 50% overlap of the interrogation areas.

Two types of image displacement fields are studied in the simulation tests: uniform displacement $\Delta X_0 = (\Delta X_0, \Delta Y_0)$ and uniform displacement superimposed onto a sinusoidally-varying displacement given by

$$\Delta\mathbf{X}(X,Y) = \left(\Delta X_0 + a\sin\left(\frac{2\pi X}{\lambda}\right)\sin\left(\frac{2\pi Y}{\lambda}\right),\right.$$
$$\left.\Delta Y_0 + a\cos\left(\frac{2\pi X}{\lambda}\right)\cdot\cos\left(\frac{2\pi Y}{\lambda}\right)\right) \qquad (13)$$

In the case of uniform displacement, the magnitude of the displacement $\Delta l = |\Delta X_0|$, is varied from 10 to 30% of the interrogation-spot size. In the case of sinusoidally-varying displacement, the uniform displacement is fixed at 10% (25.6 pixels) of the interrogation-spot size, and the amplitude of the sinusoidal motion, a, is varied from 10 to 30% of the uniform displacement, Δl. Additionally, the wavelength of the motion, λ, is varied from $0.5d_I$ to $4d_I$ to assess the spatial frequency response of the super-resolution algorithm.

The results of the simulation are shown in Figs. 2–5. The probability of success of the super-resolution-KC method is shown as a function of the particle-image

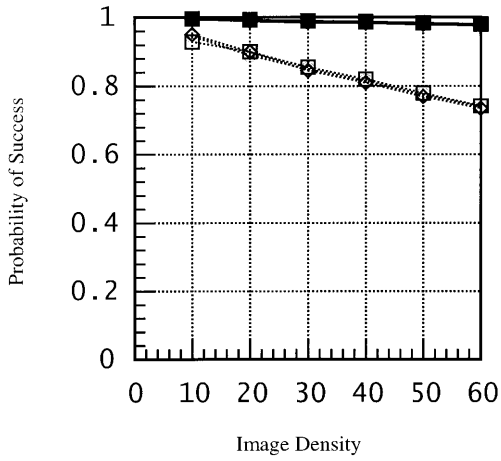

Fig. 2. Probability of a successful measurement as a function of the image density, N_I for various uniform displacements. ● $\Delta l = |\Delta X_0| = 25.6$ pixels, ◆ $\Delta l = 51.2$ pixels, ■ $\Delta l = 76.8$ pixels, ○ Keane et al. (1995)

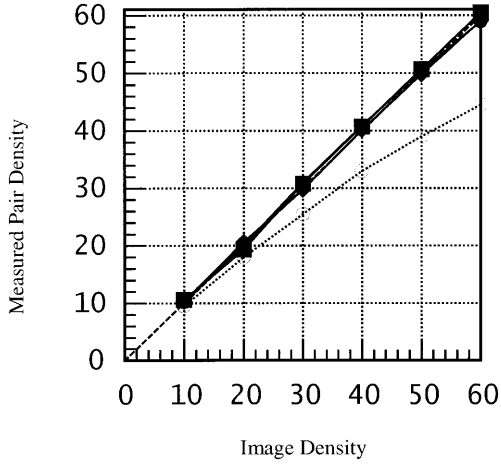

Fig. 3. Mean number of successfully measured image pairs versus image density for various uniform displacements. Symbols as in Fig. 2

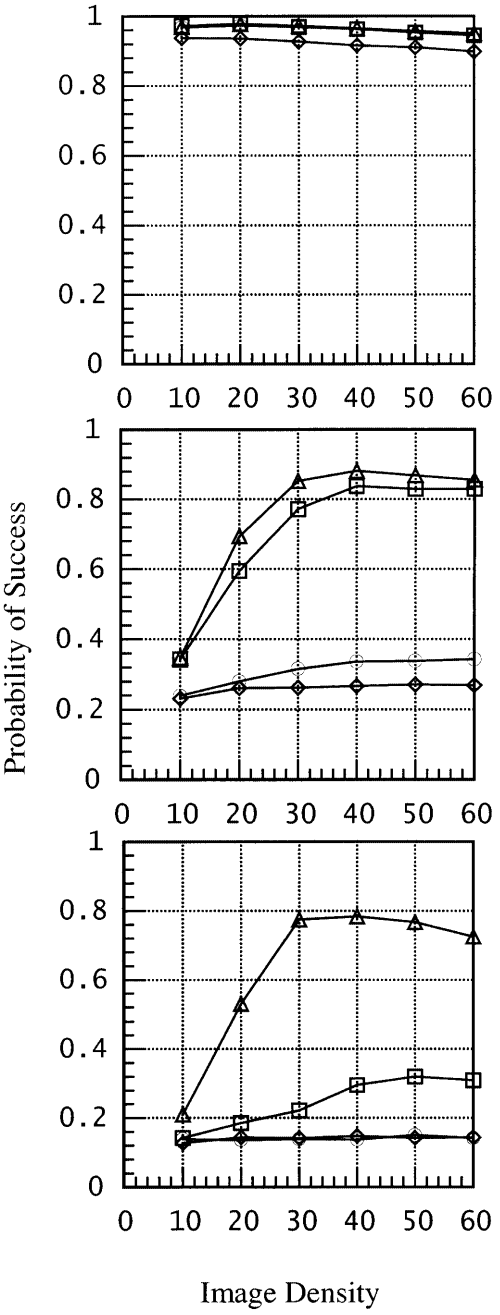

Fig. 4. Probability of successful measurement versus image displacement for the case of a velocity field varying sinusoidally with amplitude a and various wavelengths λ. $\Delta l = 25.6$ pixels. **a** $a = 0.1\Delta l$, **b** $a = 0.2\Delta l$, **c** $a = 0.3\Delta l$. ◆ $\lambda = 1/2\mathrm{d}_I$, ○ $\lambda = \mathrm{d}_I$, $\lambda = 2\mathrm{d}_I$, $\Delta\lambda = 4\mathrm{d}_I$. This "sine-wave-test" gives the spatial frequency response of the PIV in the usual sense

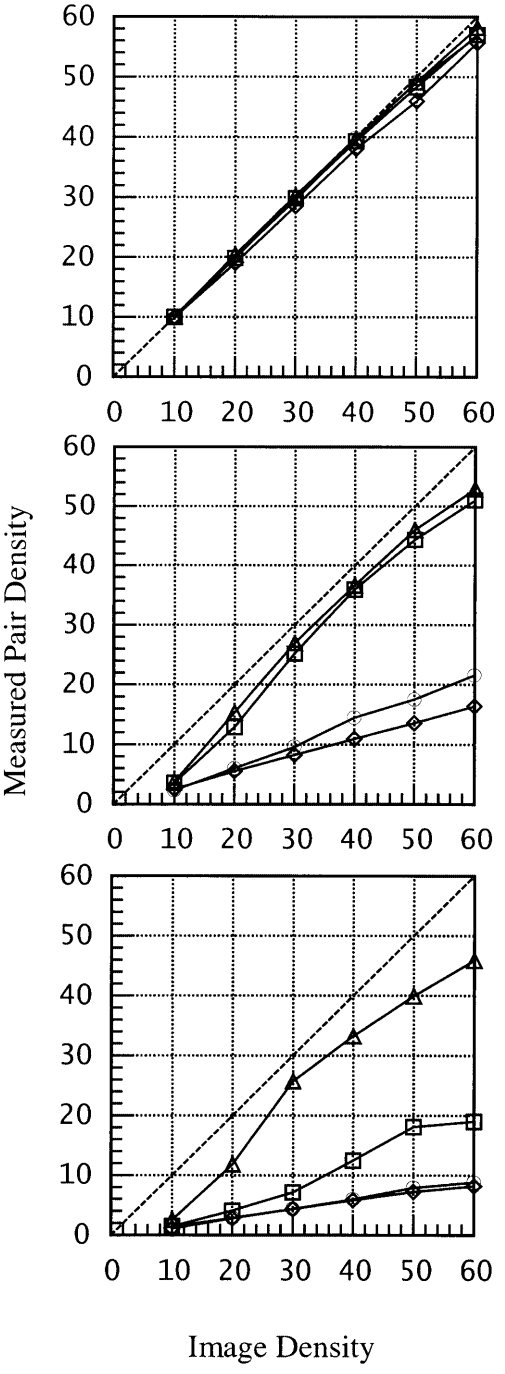

Fig. 5. Mean number of successful measurements versus image displacement for the case of a velocity field varying sinusoidally with amplitude a and wavelength λ. $\Delta l = 25.6$ pixels. **a** $a = 0.1\Delta l$, **b** $a = 0.2\Delta l$, **c** $a = 0.3\Delta l$. Symbols as in Fig. 4. This "sine-wave-test" gives the spatial frequency response of the PIV in the usual sense

density in Figs. 2 and 4. Probability of success is defined as the ratio of the number of correctly-identified particle-image pairs to the number of measured particle pairs. Figures 3 and 5 illustrate the corresponding measured particle pair density (i.e. the mean number of vectors measured successfully per interrogation spot) with regard to the particle-image density.

The results of the uniform displacement analysis are shown in Figs. 2 and 3. For reference, the open circles, diamonds, and squares represent the results of Keane et al. (1995). As mentioned earlier, the latter method began with a correlation analysis that was followed by a simple nearest neighbors search to find the correct particle pairings. It achieved a success rate of 70–90%, with the rate of success decreasing with increasing image density. Hence, if one added particles to the flow to increase the mean number of measurements, the nearest neighbors routine became confused by the rapidly-increasing number of possible

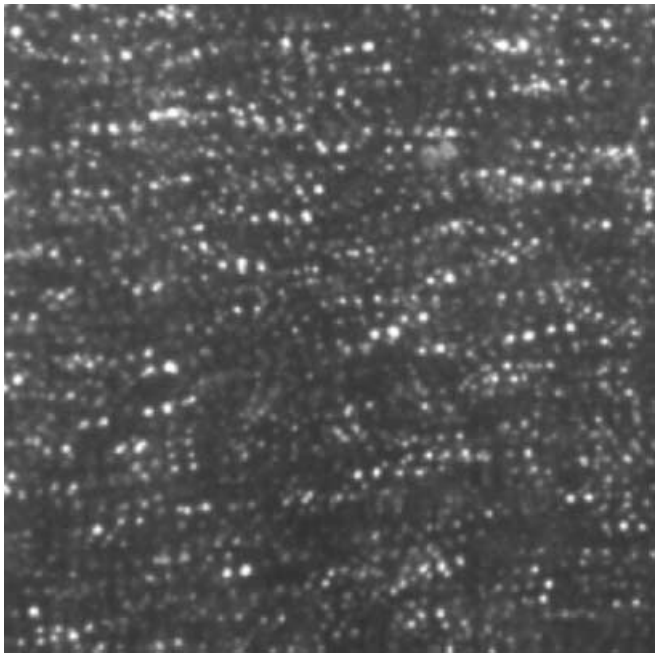

Fig. 6. Typical double-pulse/single-frame image from the water tank experiment

pairings. Further, as the concentration is increased, the spacing between images decreases, leading to frequent failure of the nearest neighbors criterion in identifying particle-image pairs belonging to the same particle. In contrast, the super-resolution-KC method correctly pairs almost all of the images at any particle-image density. The particle-pair density measured by the super-resolution-KC method is exactly the same as the particle-image density (Fig. 3). These results show great improvement of the super-resolution-KC method over the original super-resolution method of Keane et al. (1995).

The super resolution technique, in almost all forms, becomes more susceptible to failure when the velocity field changes rapidly, chiefly because the algorithm cannot rely upon local average behavior to guide proper selection of particle pairs. Results for the case of sinusoidal motion of amplitude $0.1\Delta l$ show little of this effect (Fig. 4a), but increasing the amplitude to $0.2\Delta l$ and $0.3\Delta l$ causes the success rate to drop below normal levels (Fig. 4a, b, respectively).

In the worst case, when the amplitude of the sinusoidal motion is $0.3\Delta l$, the particle-image density is higher than 30, and the wavelength of the sinusoidal motion is larger than $4d_I$, the probability of success still remains over 70%,

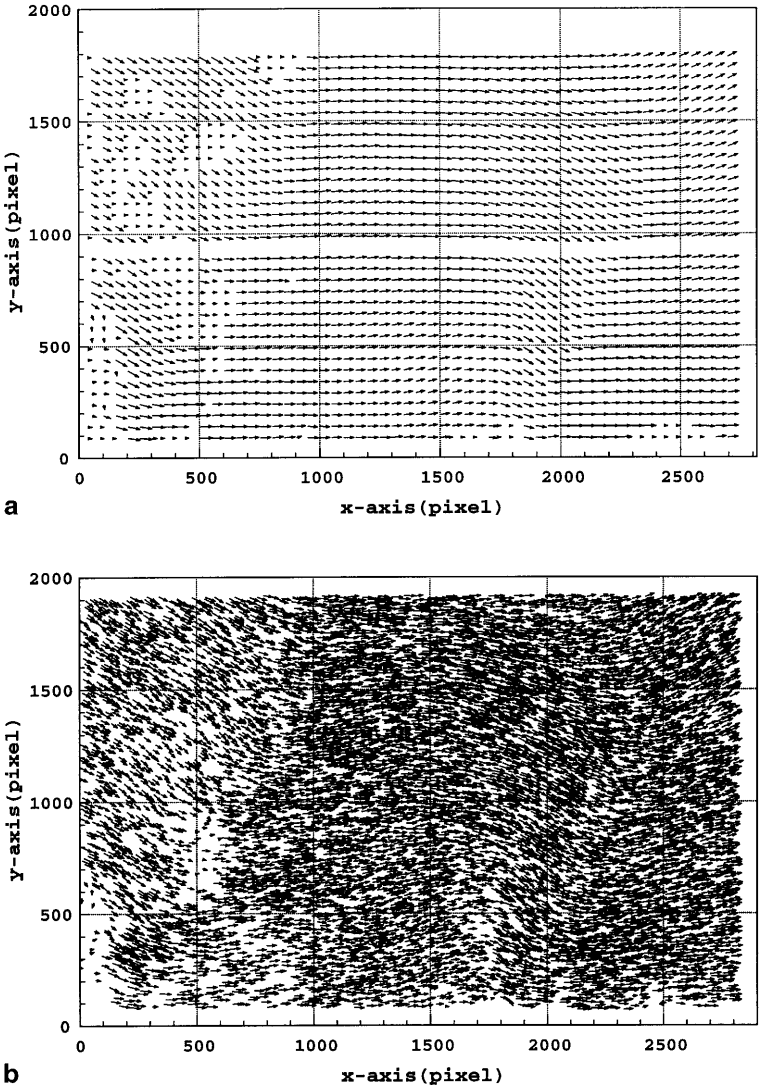

Fig. 7. Velocity measurements of a double-pulse/single-frame image obtained in the water tank experiment. **a** Vector field obtained by standard PIV analysis, **b** vector field obtained by the super-resolution-KC method

as does the measured pair density (Figs. 4c and 5c). When the amplitude of the sinusoidal motion is 20–30% of the uniform displacement, the accuracy of the super-resolution-KC method decreases with decreasing wavelength and particle-image density.

4 Application

4.1 Double-pulse/single-frame case

A double-pulse/single-frame image is analyzed to measure the velocity vector field using the super-resolution KC method. The images were recorded on 4 × 5 inch film and the film was digitized in 6 parts by a CCD camera with a resolution of 522 × 522 pixels. The measurement is of flow in a water tank. An example of the digitized image is shown in Fig. 6. Each digitized image was analyzed separately using the super-resolution KC method; however, the resulting vector fields were combined to form a single realization.

The results from analysis of this double-pulse/single-frame image is presented in Fig. 7. The velocity field obtained by standard correlation-based PIV is shown in Fig. 7a. This analysis yielded 1802 vectors. The result of standard correlation-based PIV was then used as the initial estimate in the super-resolution KC analysis. The result of the super resolution KC method is shown Fig. 7b. The number of vectors obtained by the super-resolution KC analysis is 8479, which is about 4.7 times higher than that from the standard PIV analysis.

4.2 Single-pulse/double-frame case

The super-resolution KC method was also applied to measurement of the flow field associated with a Rushton turbine. The experiment was carried out by Sharp et al. (1998) and a schematic of the experimental set-up is shown in Fig. 8. The particle images were captured using a cross-correlation CCD camera (TSI PIV Cam 10–30) with a resolution of 1K × 1K pixels. A double-pulsed Nd:Yag laser was used for illumination.

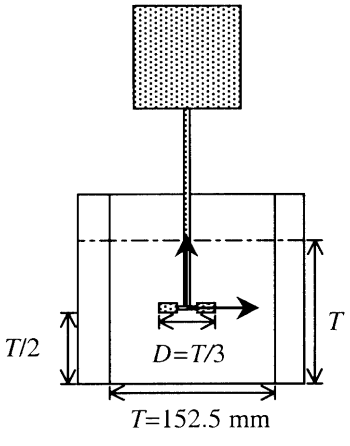

Fig. 8. Experimental schematic of the Rushton turbine experiment

The single-pulse/double-frame images acquired in this experiment were used to illustrate the robustness of the super-resolution KC method in measuring a highly-turbulent flow field. First, the two images were processed using the PMC method to extract the particle images from the data. Then, a coarse grid velocity field was computed using standard cross-correlation analysis. The first and second interrogation windows were 24 × 24 pixels and 32 × 32 pixels, respectively. The resulting PIV vector field is shown in Fig. 9a.

The velocity at each particle position was then interpolated from the coarse-grid velocity field obtained above using a Gaussian-weighted averaging operation. The calculated velocity was then used as initial estimate for the Kalman filtering, and the particles were then tracked. The super-resolution KC method results are shown in Fig. 9b.

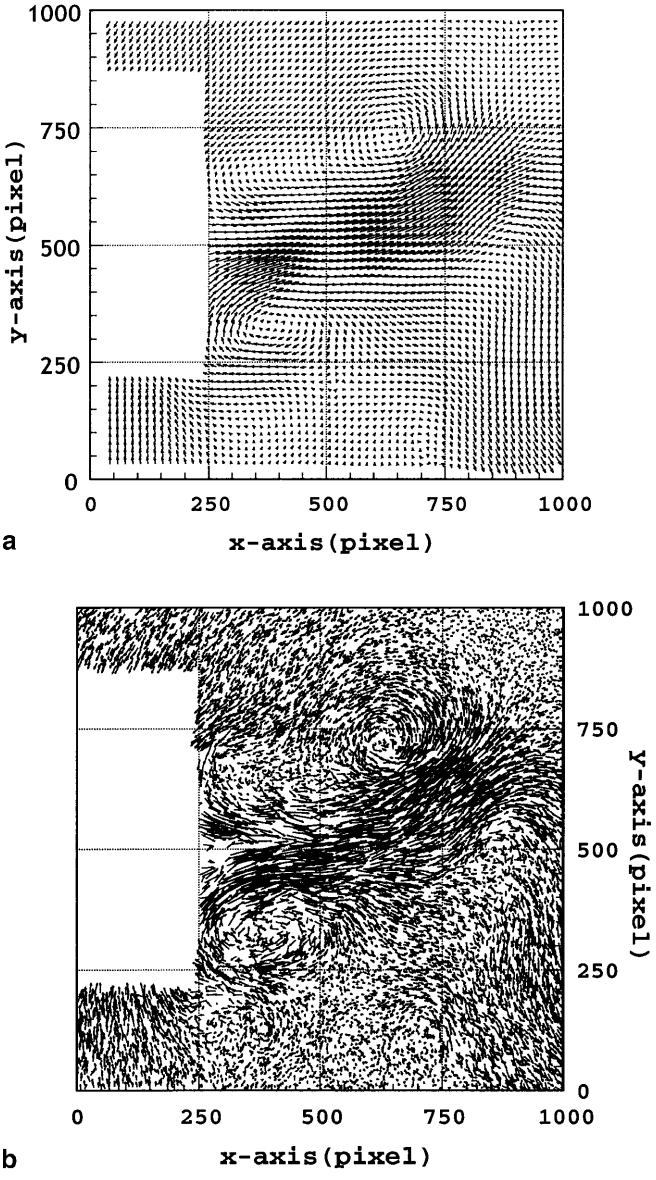

Fig. 9. Velocity measurements of a single-pulse/double-frame image (flow in the Rushton turbine). **a** Course-grid vector field obtained by standard PIV analysis, **b** velocity vector field obtained by the super-resolution-KC method

The number of vectors obtained by the cross-correlation analysis is 3067, while the number found by the super-resolution-KC method is 9204, a factor of three increase.

5 Conclusions

A new super-resolution methodology, the super-resolution-KC method, is described and evaluated. The method is a combination of the particle mask correlation method, standard PIV correlation analysis and the χ^2-method. The PMC extracts particle images from the image plane and locates their centroids accurately, the PIV correlation analysis provides a coarse-grid estimate of the velocity field, and the KC method accurately pairs particle images between the two time steps.

The performance of the super-resolution-KC method is tested by artificial particle images created by Monte Carlo simulation. Two cases of particle motion are tested: uniform displacements and sinusoidal motions superimposed on a uniform displacement. For the uniform displacement of particles, every particle can be traced correctly for any seeding density. When the amplitude of the sinusoidal motion is 10% of the uniform displacement, every particle can be traced with the accuracy of more than 95%. Finally, when the amplitude of the sinusoidal motion is 20 to 30% of the uniform displacement, the accuracy of the super-resolution-KC method decreases with decreasing wavelength of the sinusoidal motion and increasing particle-image density.

The super-resolution-KC method has also been applied to the measurement of the highly-turbulent flow field associated with a the Rushton turbine. The velocity vectors obtained by the super-resolution-KC method total about 9000, which is about three times larger than that obtained by standard PIV analysis with 50% overlapped interrogation regions.

In summary, the Kalman filtering method of tracking particle images is reliable and robust. Benchmark timing tests indicate that the computation time per vector is approximately twice the time per vector of standard correlation analysis.

References

Adrian RJ; Yao CS (1984) Application of pulsed laser technique to liquid and gaseous flows and the scattering power of seed materials. Appl Optics 24: 44–52

Etoh T; Takehara K (1990) A new algorithm for automatic tracing of particles (in Japanese). Ann J Hydraul Engr, JSCE 34: 689–694

Etoh T; Takehara K (1995) Development of a new algorithm and supporting technologies for PTV. Proceedings of the International Workshop on PIV, Fukui, Japan 91–106

Hart DP (1998) Super-resolution PIV by recursive local-correlation. Proc VSJ–SPIE98, AB149: 1–10

Keane RD; Adrian RJ (1992) Theory of cross-correlation analysis of PIV images. Appl Sci Res 49: 191–215

Keane RD; Adrian RJ; Zhang Y (1995) Super-resolution particle imaging velocity. Meas Sci Technol 6: 754–768

Prasad AK; Adrian RJ; Landreth CC; Offutt PW (1992) Effect of resolution on the speed and accuracy of particle image velocimetry interrogation. Exp Fluids 13: 105–116

Sharp KV; Kim KC; Adrian RJ (2000) Dissipation estimation around a Rushton turbine using particle image velocimetry. In: Adrian R et al. (eds), Laser techniques for fluid mechanics. Springer, Berlin Heidelberg New York

Takehara K; Etoh T (1999) A study on particle identification in PTV – particle mask correlation method. J Visualization 1: 313–323